



Title	Bulk Metallic Glass Multiscale Tooling for Molding of Polymers with Micro to Nano Features : A Review
Authors(s)	Browne, David J., Stratton, Dermot, Gilchrist, M. D., Byrne, Cormac J.
Publication date	2012-09-27
Publication information	Browne, David J., Dermot Stratton, M. D. Gilchrist, and Cormac J. Byrne. "Bulk Metallic Glass Multiscale Tooling for Molding of Polymers with Micro to Nano Features : A Review" 44, no. 5 (September 27, 2012).
Publisher	Springer-Verlag
Item record/more information	http://hdl.handle.net/10197/4846
Publisher's statement	The final publication is available at www.springerlink.com
Publisher's version (DOI)	10.1007/s11661-012-1427-7

Downloaded 2023-10-05T14:16:07Z

The UCD community has made this article openly available. Please share how this access benefits you. Your story matters! (@ucd_oa)



© Some rights reserved. For more information

Bulk Metallic Glass Multi-Scale Tooling for Molding of Polymers with Micro to Nano Features: a Review

D.J. Browne, D. Stratton, M.D. Gilchrist, C. Byrne

School of Mechanical & Materials Engineering

University College Dublin

Abstract

There is a growing demand for single-use disposable polymer devices with features at sub-micron scales. This requires resilient tooling which can be patterned to scales of the order of hundreds of nm. The requisite topology can be imparted to silicon but it is too brittle to be of use in a die to mold thousands of plastic parts. The polycrystalline nature of tool steel means it cannot be patterned with sub-micron detail. Some bulk amorphous alloys have the requisite mechanical properties to be viable as materials for such dies, and can be patterned – e.g. via embossing as a supercooled liquid into MEMS silicon or using FIB – with sub-micron features which may persevere over many thousands of molding cycles. The composition of the amorphous alloy must be carefully selected to suit the particular molding application (polymer/process). The state-of-the-art of is presented, along with results of our recent experimental investigations.

I. Introduction

Injection molding is a long-established process for manufacture of polymer components, of sizes 10^{-3} to 10^0 m, and with surface features as fine as 10^{-4} m. However there is a growing market for components for microengineering applications or for multi-scale components in the 10^{-3} to 10^{-1} m size range with sub-micron surface features. The major applications are for MEMS sensors and microfluidic devices [1]. The global microfluidics market in 2009 was estimated at \$2.1 b, growing at 13.5% p.a. [1]. Polymer is and will remain the main substrate for microfluidic applications, and the market size for plastic microfluidics alone is forecast to be worth \$2.5 b by 2016 [2], and clinical point-of-care diagnostics will account for 75% of this. For these reasons, this paper is primarily concerned with enabling technology for production of the single use disposable microfluidic Lab-on-Chip (LoC) chemical and biochemical analysis devices needed for such diagnostic applications. As the devices will be used for rapid diagnosis on-site at, for example, a general medical practise, they will need to be mass-produced and of an inexpensive material: they will be of injection molded polymer. There is therefore a need to develop durable tooling in which to mold such polymer micro-bio-chips invested with the fine features available via lithography to silicon and glass. Other applications for molded components with surface features down to 10^{-5} m in size include microlens arrays for LED illumination [3] and micro-gears [4]. In life science applications, molded LoC devices will be required with surface features of detail finer than the 10^{-5} m representative of a red blood cell – i.e. further down the “biological ruler” [5].

II. Tooling requirements

The current generation of microfluidic devices have channel dimensions in the tens to hundreds of μm range. The requisite mold tool materials need to be amenable to being micro-machined to produce such patterns in negative, and must be resilient i.e. resistant to wear or other forms of surface or structural degradation, including those relating to thermal fatigue, over several thousands of molding cycles. However, tool steel – the workhorse of traditional injection mold tooling – is finding its limits in terms of minimum feature size as the number of microns in the scale becomes small [6]. This is due to the polycrystalline nature of tool steel, where even in the fine-grained alloys when the size of the surface feature gets down to the grain size then grain boundary and crystallographic misorientation effects start to interfere with the desired surface pattern.

However the demands on tooling materials are ever-increasing as the need to produce and replicate patterns of ever-increasing resolution emerges. In the LoC life science applications this is due to the incorporation of features representative of cell (10^{-5} m), bacterium (10^{-6} m) and even virus (10^{-7} m) into microfluidic chips. The next generation of microfluidic devices thus have to be patterned with sub-micron features yet their overall dimensions must be those of industry standards [7] established to assist interconnection and performance for microfluidic interfaces and to enable low cost and high volume manufacturing of products. A typical standard microfluidic chip will be of credit card size – i.e. a few cm^2 . What is needed then, is multi-scale tooling for molding new LoC components.

The manufacturing processes will be micro-injection molding, compression-injection molding, or hot embossing [8].

Micro-injection moulding can be used to manufacture polymer components with complex shapes and high quality surface features, similarly to conventional injection moulding [5]. However, the process differs significantly from the conventional process since micro parts and micro/nano features have very high surface to volume ratios, which means that heat diffusion effects are significant [9,10]. This means that the polymer melt solidifies more quickly than in conventional injection moulding. Elevated temperatures and higher pressures are usually required to force the polymer melt into micro cavities as quickly as possible. This causes polymer melt to experience very high shear rates and very high thermal gradients during micro injection molding. Melt rheology under such extreme conditions controls the polymer flow behavior at the micro/nano meter scale.

Unique morphological features and lower mechanical properties than those reported for conventional parts have been reported for micro injection molding [11]. It is also reported that the quality of micro components is very sensitive to process variations [12]

III. Candidate Tool Materials

Although designed for durability, tool steel cannot be patterned to the requisite sub-micron resolution due to limitations relating to its finite grain size. Silicon, on the other hand, can be patterned with sub-micron features via lithography and etching – a fact which has made it the

first material of choice for MEMS devices. The fracture toughness of silicon is, however, insufficient for direct use as a mold tool material [13] and it fractures after just a few molding cycles. For manufacture of CDs and DVDs, laser beam recording is used to pattern, with sub-micron features, a glass disc by photolithography. The glass master is then electroplated with nickel to produce a thin metal template known as a stamper. This patterned shim needs to be backed up to provide sufficient support for use in the die employed for injection molding of the polycarbonate optical discs. Electroplating of nickel or nickel-cobalt alloy onto MEMS-Si has been used to create a negative impression of a Si master, albeit a thin one without a planar back side. However the Si master needs to be pre-treated [8] by cleaning and deposition of a thin layer of Ti/Cu by PVD, or of Ni by electron beam evaporation [14]. Following the electrodeposition of the Ni alloy, the Si master must be etched away in a warm alkaline solution. Such a flimsy electroplated sheet also needs to be backed up mechanically for rigidity in molding, and the manufacturing process is slow and expensive.

Engineers have been looking for alternative mold tool materials due to the limitations of the existing candidates, and bulk metallic glasses are attractive in that they can be patterned with features of sub-micron size, they are durable and wear-resistant, and they can be fabricated in bulk form i.e. with section sizes 10^{-3} to 10^{-2} m. Metallic glasses are amorphous alloys and so there are no lower limits on feature size imposed by crystallinity. Metallic glasses also have high compressive strength (generally exceeding that of conventional alloys) and have high hardness and wear resistance. Bulk Metallic Glasses (BMGs) thus overcome the key limitations of its main rivals for micr-nano mold tools: steel, silicon, and nickel electroform.

IV. Fabrication and Use of Bulk Metallic Glass Tools

Direct casting of tools

Direct casting of conventional crystalline metal tools with small features is challenging if not impossible below certain length scales due to volume shrinkage associated with crystallisation. Secondary machining/forming is always required to achieve a high surface finish or to pattern the surface of the cast material. BMGs on the other hand undergo very little volume shrinkage on cooling from the liquid phase and because of their amorphous structure are better able replicate small features which may be present on the mold wall. However challenges exist and net-shape casting of tools with 10^{-8} to 10^{-5} meter scale features is unlikely to be possible. Obstacles include: (1) the need to produce a precision featured, high temperature (able to operate at $>500^{\circ}\text{C}$) master casting mould which itself will be subject to significant volume change during heating and cooling; (2) the increasing dominance of capillary effects at small scale [15] which will resist the liquid metal flowing into small features; and (3) the need to be able to remove the cast part from the mould without damaging small features [13].

However advances in casting techniques for large sectioned BMGs are likely to make near-net shape casting of BMGs with 10^{-4} to 10^{-2} m scale features possible [16]. Smaller features may then be added to these near-net shape cast BMGs using more sophisticated machining techniques (outlined below). This will allow the creation of multi-scale BMG tools for molding of polymers.

Melt spinning techniques, which have been widely used for the past 40 years to produce thin amorphous ribbons, can be used to pattern the ribbon via direct or indirect patterning of the

melt-spinning wheel. The smallest scale features replicable using this technique are likely to be approximately 100 μm [17] but the fidelity of replication is not expected to be good quality. Thus incorporation of these thin ribbons into tools for patterning polymers is unlikely to be of practical use. However advances in twin roll casting of BMGs may offer possibilities for producing larger dimensioned, flat sections [18-20]. The technique, even if matured sufficiently, will inevitably suffer from feature size limitations similar to single roller techniques. But twin-rolling is an attractive route for high-volume (continuous) manufacture of near-net shape BMG feedstock for secondary processing via additional techniques outlined later.

The authors are unaware of directly cast BMG tools with micron (or smaller) scale features having being used for embossing or injection moulding of polymeric components.

Thermoplastic forming

Perhaps the most widely explored method of micro- and nano- patterning BMGs is that of thermoplastic forming. When heated above their glass transition temperature but below their crystallisation temperature the viscosity of BMGs drops considerably such that the glass flows readily [21]. In this state the BMG can be molded or formed to shapes with features on the order of nanometers [22] using only moderate forces. Once cooled again below the glass transition temperature the BMG becomes solid and the forming and features are frozen in place. There is no reduction in mechanical properties during this forming process, so the BMG substrate retains its strength after forming.

The limits of conventional machining – i.e. by mechanical removal of materials – of crystalline alloys for use as masters for embossing BMGs has been explored by Pan and co-workers [23,24]. Precision machining, including computer numerical control optical projection grinding, lapping, and polishing, was used [23] to fabricate a W-steel mold with triangular-pyramidal patterns of minimum feature size of about 100 microns. A diamond grinding wheel of knife type was used; the tool radius was 25 microns. To manufacture PMMA optical film with a similar pattern, an intermediate step of developing a MgCuY BMG working tool via hot embossing onto the W-steel mold was used. Blank PMMA film was then hot embossed onto the durable BMG mold. A similar approach was taken in the manufacture of an aspheric PMMA lens [24]: conventional micromachining of a copper mold was followed by hot embossing with BMG to provide a mold harder than the copper master, and the BMG mold was in turn used in hot embossing the PMMA. A PMMA array of micro-lenses each 140 microns in diameter was also produced reasonably successfully in this work.

Whilst moulding into crystalline metal dies allows small components to be manufactured [25], the addition of micrometer and smaller features requires the application of more sophisticated methods. A well known method of creating BMGs with micrometer and nanometer scale features is to thermoplastically form the BMG using a silicon master mould [4,26,27]. The manufacturing route for thermoplastic forming of BMGs by silicon embossing is outlined in Fig. 1. In this case the Si wafer mould is first patterned using standard lithography and deep reactive ion etching (DRIE) process. The BMG and silicon package are then heated above the glass transition temperature of the BMG and the BMG is pressed into the silicon in order to replicate the silicon's features onto the BMG. The pressing operation can be delicate due to the brittleness of the silicon wafer. The package is then cooled and the silicon typically dissolved away using potassium hydroxide [4,27,28]. Given the right

processing conditions the resulting micro/nano patterned BMG then has the potential to be used as a robust metallic tool for forming many polymeric components with micro/nano-scale features. Alternatively features may not be desired (optically smooth surfaces for example) and in such case a BMG may serve as a robust tool for creating such a smooth, featureless surface [29].

The challenges associated with the use of a silicon master mould are cost and the usually sacrificial nature of the silicon master. However the scale and fidelity of replication which can be achieved is impressive [30] and the BMG tools formed can be used to produce thousands of polymeric components. Furthermore, through the addition of an extra processing step, value can be added to Si-master moulds. An example is shown in Fig.2. In this case the Si master is used to produce a high T_g BMG sub-master which can then be used to emboss multiple lower T_g BMG tools [28]. Using this route one silicon master can generate many more polymeric components albeit with a more complicated manufacturing route and a more limited choice of BMG alloys for the tool as it is necessary to have a second BMG with a lower glass transition temperature than the first.

Other thermoplastic master moulding routes have been used to form micrometer and sub-micrometer scale features on BMGs. Pan *et al.* have formed features on Si wafer using lithography methods [3] and then electroplated this with Ni and formed a micro-lens array on BMG from the resultant master. Pryds used this method [31] to replicate a sine pattern with wavelength of $1\mu\text{m}$ and trough to crest distance of approximately 160 nm in an amorphous MgCuY alloy. Features down to 13nm in length have been reproduced by embossing a BMG using porous alumina [22]. This work has set a benchmark in the field of thermoplastic forming of BMGs, and has recently been extended [32] to develop BMG nanowire architectures for high performance catalysis. Other, novel thermoplastic forming routes such as blow moulding [33] or injection molding [34] may offer ways of producing 3-dimensional BMG tools from Si-incorporated masters.

Direct Machining (Normal, Laser, EDM, Electrochemical, FIB)

Direct machining of features onto bulk metallic glass is the most direct means of manufacturing a multi-scale tool. Generally metallic glasses are considered relatively brittle, although some newly developed alloys based on noble metals show extraordinarily high toughness [35,36]. Other studies have shown that certain BMGs, including Zr-based alloys, can be machined using conventional techniques such as milling or turning [37,38]. Such bulk methods allow large scale features to be machined rapidly onto a BMG, but cannot typically create features less than several hundred micrometers. More sophisticated machining techniques are required to allow features in the range 10^{-9} m to 10^{-5} m to be placed on a tool

We have shown wire electrical discharge machining (wire-EDM) to be able to produce features with length scale of order $100\mu\text{m}$ (Fig.3). EDM using a tip tool has also shown similar results [39]. In both cases the quality of the surface finish tends to be poor.

Other techniques, though requiring maturation, have been shown to be possible for use in machining features of order 10^{-5} m onto at least Zr-based BMGs. Novel electrochemical micromachining of holes in Zr-based BMG has been demonstrated [40]. Other authors have demonstrated the feasibility of using laser cutting to feature BMGs [41] although the resulting ‘troughs’ have a poor surface finish and it is difficult to see a means of improving

the surface finish. Laser drilling of holes and machining of trenches in amorphous $Zr_{47}Cu_{45}Al_8$ and $Zr_{47}Cu_{45}Al_8Ag_8$ samples from the authors' laboratory are shown in Fig. 4(a) and (b).

Focused Ion Beam (FIB) machining of BMGs allows very precise features to be placed on the surface of the BMG [42]. FIB operates on the principle of directing a beam of gallium ions at the surface of the material in order to mill away material given a sufficiently high beam current. Features ranging from micrometers to nanometers can be milled in BMGs using this technique. The disadvantage is the length of time taken to mill a given area. Currently it is not practical to machine mm^2 areas. However precisely defined sub-micron features can be added to an already grossly machined tool to add value to the tool.

The benefit of FIB machining of BMGs as opposed to crystalline metals can be seen in Fig. 5. Where BMGs are machined the patterns are sharp. In the case of the crystalline metals it is not possible to mill features at these length scales.

FIB machining has been used extensively by the authors to manufacture BMG tools with micrometer and nanometer scale features.

V. Current Research

Choice of BMG alloy

The authors have been working on developing technology for micro-nano-patterning of polymers via BMG tooling. One of the first tasks was selection of a suitable alloy composition. The Cu-Zr-Al system was chosen due to its good GFA, lack of toxic or prohibitively expensive elements, and reasonable high glass transition and service temperatures, enabling use for molding a variety of polymers. For example, the measured compression strength of $Zr_{47}Cu_{45}Al_8$ was 1678 MPa, and with a hardness of 500 H_v is very suitable as a durable wear-resistant die material. Similar mechanical properties have been reported [43] for a BMG alloy of composition close to that tested for use by the current authors. The glass transition temperature was measured as 715 K, and a silver containing variant, $Zr_{44}Cu_{40}Al_8Ag_8$ has a T_g of 721 K. Following wear tests, devitrification studies, and FIB machining trials (see Fig. 5) it was decided that these alloys had the correct balance of properties, including thermal stability, for multi-scale tooling applications. All BMG cylindrical ingots (typical diameter 5 mm) for this work were cast, using high purity metallic components, into copper molds in an arc melter, under an argon atmosphere. The ingots were then machined to the desired shape, then ground and polished to be ready for patterning.

Micro injection molding

Samples of the $Zr_{47}Cu_{45}Al_8$ BMG alloy were prepared as inserts for a steel die for use in micro injection molding [5]. Using FIB milling, arrays of pillars and holes, with diameter down to 100 nm and depth to 200 nm, were created on the surface of the BMG insert. Micro injection molding using HDPE showed that these features were replicated, albeit not to full depth, in the surface of HDPE components [5].

Fig. 6.(a) shows, by way of example, the sub-micron 7 x7 array of BMG pillars inside a 3 x 3 μm cavity and, in Fig. 6(b) the replication of these surface features as an array of submicroscopic holes on the micro injection molded HDPE part is illustrated. Further optimisation of the machine parameters (such as injection pressure and mold temperature) is needed to improve feature filling by the molten HDPE. In another series of tests [5] to establish the capability for generating ultra-smooth surfaces, strips of BMG were polished to $R_a \leq 8\text{nm}$ and placed as inserts in a different set of steel dies and used for micro-injection molding of PMMA plates. The plates replicated the mirror surface finish, and the resultant excellent local optical clarity is useful in LoC applications.

In other work the sensitivity of filling success to the direction of flow of the polymer melt was investigated [10]. Two sets of channels and ridges of, respectively, depth or height 2 μm were FIB machined into the BMG insert. Channel widths ranged from 0.3 to 4.0 μm and ridge widths from 0.45 to 4.0 μm . One such set of linear patterns was aligned with the flow direction, one perpendicular to the flow direction, in the micro injection molding of HDPE polymer. After a design of experiments study, to establish optimum injection molding parameter settings, it was found that ridge features aligned with the flow directions showed best replication in the polymer part, but that orientation had a smaller effect on the channel features. [10], as per Fig. 7. This finding is important in the design of parts with surface features of the order of one micron. The BMG die insert was found to last over several thousand cycles of molding.

Hot Embossing

If it is not necessary to manufacture a 3D plastic component to near net shape with surface micro-nano-features, embossing is an option for simply transferring a fine pattern from BMG mold tool to a flat sheet of polymer. Trials were carried out to develop a Zr44 Cu40 Al8 Ag8 BMG embossing tool. It has been shown [44] that addition of Ag to the Zr-Cu-Al alloy improves its oxidation resistance. A 5 mm diameter cast cylinder was firstly cut into thin discs of 5 mm height using a high-speed diamond saw [6]. These sections were then compressed, within their SCL temperature range, into ~10 mm diameter by ~1 mm thick discs using a heated platen set-up mounted onto a universal testing machine. The resulting discs were then polished to a .05 micron finish. The amorphous nature of these discs was verified by differential scanning calorimetry (DSC) and X-ray diffraction (XRD). The discs were then milled using a focused ion beam in a FEI Quanta 3D FEG DualBeam SEM. The BMG discs with milled sub-microfluidic patterns and micro-UCD crest were then used as dies and pressed into 0.5 mm PMMA sheet at varying temperatures and pressures using the heated platen set-up referenced above [6]. The BMG die and PMMA sheet were placed on the platens at embossing temperature above the T_g of the PMMA, but well below the T_g of the BMG, and allowed to equilibrate to this temperature for 60 seconds before pressure was applied. This pressure was held for 3 minutes before the heaters were turned off. The pressure was then held between the mold and PMMA and air-cooled to below 90°C. The average cooling rate was approximately 5°C/min, so total holding time varied, depending on the embossing temperature used. A Design of Experiments approach was taken, in which embossing temperature and pressure were systematically varied, with replication results as shown in Fig.8. The optimal processing conditions were determined to be a temperature of 120°C with a pressure of 2.5 MPa.

As noted in section IV, hot embossing may also be used in order to impart patterns on the BMG substrate itself. In this approach patterns are imparted on a master mold and then the BMG material is thermoplastically formed into master mold. This BMG mold can then be used for the hot embossing of a polymeric material that exactly replicates the shape and structure of the initial master mold. If a scaleable patterning technique can be used on the master mold, then the entire process can also be scaled. This removes the limitation of the small surface area limitations of the FIB patterning technique. For this study, a silicon master mould was created via standard optical lithography and DRIE technique. Vitreloy 1b, a BMG alloy commercially available from Liquidmetal Technologies, Rancho Santa Margarita, CA, USA, was then embossed into this Si master mould and PMMA was then hot embossed into this BMG die. The starting BMG substrate represents a surface area that is orders of magnitude higher than that which is feasible with the FIB milling approach.

Fig.9 shows white light interferometer (WLI) images of the entire BMG hot embossing process. Two different starting master molds are represented. The first – see column of Fig. 9(a) is patterned with large octagonal structures, 30 μm wide and 3 μm deep, randomly placed across the Si chip. The second – Fig. 9(b) also features Large octagonal structures, 30 μm wide and 3 μm deep, but with with superimposed small octagonal structures, 3 μm wide and 1 μm deep randomly placed across the chip. Each molding process starts with a silicon master mould prepared via optical lithography and deep reactive ion etching (DRIE). The silicon masters features are displayed in the first row of Figure 2. Both these molds were embossed into a BMG (Vitreloy 1b) using a custom designed hot embossing machine with a pressure of 40 MPa at a temperature of 478 $^{\circ}\text{C}$. The images in the second row of figure 2 show the WLI image of the embossed BMG. Many of the small features on the silicon were not replicated on the BMG for 2 reasons: 1) imprecise control of forming platen temperature and 2) forming occurred in air and the resulting oxidation impeded complete filling of the Si mold. Oxidation of BMGs has been shown [45] to be strongly dependent on temperature and alloy composition. For example, as stated previously, it has been established [44] that addition of Ag to Cu-Zr-Al BMGs improved their oxidation resistance and GFA, and the morphology of oxide formation has also been reported [46] for such alloys. However some of the 5 μm features are still evident inside the main circular features. A polymer, Poly(methyl methacrylate) (PMMA), was then hot embossed on the BMG tool to create a replica of the silicon master mold. A Jenoptik HEX-03 hot embossing machine was used to emboss the PMMA material. The samples were embossed with a force of 750 N and a temperature of 125 $^{\circ}\text{C}$. The third row of images are WLI images of the hot embossed polymer. Reasonable results were obtained, but future optimisation of both embossing processes should improve the replication quality.

VI. Conclusions

Following recent strong growth in research in the field BMGs have become the material of choice for durable multi-scale tooling for molding of polymer devices with overall size up to 100 mm but with surface features of scale down to 100 nm.

Acknowledgements:

The authors would like to thank Enterprise Ireland for funding this research, through contracts CFTD/07/314 & CFTD/06/IT/335. We would also like to thank Dr. Ian Reid (NIMAC-UCD) for assistance with microscopy and FIB machining. Fig 4 is courtesy NCLA Galway, Ireland. Fig. 9 is courtesy of Tyndall Institute, Cork, Ireland, under National Access Programme Grant number 275, and provided with assistance from Mr Jaap Verheggen.

References

- [1] Frost & Sullivan, “High Volume Applications for UCD’s New Micro Injection Molding Based Technology: An Opportunity Assessment”, Private Report, August 2011, Frost & Sullivan, Mountain View, CA, USA.
- [2] Yole Développement, “Microfluidic Substrates Market and Processing Trends”, Report, July 2011, Yole Développement SA, Lyon, France.
- [3] C.T. Pan, M.F. Chen, P.J. Cheng, Y.M. Hwang, S.D. Tseng and J.C. Huang, *Sensors & Actuators A*, 2009, vol. 150, pp. 156-167.
- [4] D. Wang, G. Liao, J. Pan, Z. Tang, P. Peng, L. Liu and T. Shi (2009) *J Alloys Cmpds*, 2009, vol. 484, pp. 118-122.
- [5] N. Zhang, C.J. Byrne, D.J. Browne and M.D. Gilchrist, *Materials Today*, 2012, vol.15. pp. 216-221.
- [6] D.J. Stratton, C. Byrne, J. Mulcahy and D.J. Browne, *MRS Proceedings*, 2011, vol. 1300, mrsf10-1300-u02-08.
- [7] SEMI MS9-0611 - Specification for High Density Permanent Connections Between Microfluidic Devices, SEMI Global Headquarters, San Jose, CA, USA.
- [8] H.N. Hansen, R.J. Hocken and G. Tosello, *CIRP Annals – Manufacturing Technology*, 2011, vol. 60, pp. 695-714.
- [9] N. Zhang and M.D. Gilchrist, Characterisation of thermo-rheological behaviour of polymer melts in micro injection moulding process. *Polymer Testing*. (2012) in press.
- [10] N. Zhang, J.S. Chu, C. Byrne, D.J. Browne and M.D. Gilchrist, *Journal of Micromechanics and Microengineering*, 2012, vol. 22, 065019.
- [11] M.R. Kamal, J.S. Chu, S. Derdouri and A. Hrymak, *Plast. Rubber Compos.*, 2010, vol. 39, pp. 332–341.

- [12] B.R. Whiteside, R. Spares, K. Howell, M.T. Martyn and P.D. Coates, *Plast. Rubber. Compos*, 2005, vol. 34, pp. 380–386.
- [13] C.J. Byrne, M. Eldrup, M. Ohnuma and R.S. Eriksen, *Journal of Materials Processing Technology*, 2010, vol. 210, pp. 1419–1428.
- [14] N. Lee, S-D. Moon, S. Kang and S. Ahn, *Optical Review*, 2003, Vol. 10, pp. 290-294.
- [15] S. Ding, J. Kong and J. Schroers, *J. Appl. Phys.*, 2011, vol. 110, 043508.
- [16] T. Zhang, X. Zhang, W. Zhang, F. Jia , A. Inoue, H. Hao and Y. Ma, 2011, vol. 65, pp. 2257–2260.
- [17] C. Byrne, A.M. Kueck, S.P. Baker and P.H Steen, *Mater. Sci. Eng. A*, 2007, vol. 459, pp. 172-181.
- [18] J.G. Lee et al., *Scripta Materialia*, 2005, vol. 53, pp. 693–697.
- [19] G. Duggan and D.J. Browne, *Transactions of the Indian Institute of Metals*, 2009, vol. 62, pp. 417-421.
- [20] D. East, M. Kellam, M.A. Gibson, A. Seeber, D. Liang and J.-F. Nie, *Mater. Sci. Forum*, 2010, vol. 654-656, pp. 1078-1081.
- [21] Y. Kawamura et al., *Materials Science and Engineering*, 2001, vol. A304–306, pp. 674–678.
- [22] G. Kumar, H.X. Tang and J. Schroers, *Nature*, 2009, vol. 457, pp. 868-872.
- [23] C.F. Liu, C.T. Pan, K.H. Liu, Y.C. Chen, J.L. Chen, and J.C. Huang, *J. Materials Engineering & Performance* 20 (2011) pp. 1544-1553.
- [24] C.T. Pan, T.T. Wu, Y.T. Liu, Y. Yamagata and J.C. Huang, *Journal of Materials Processing Technology*, 2009, vol. 209, pp. 5014–5023.
- [25] J. A. Wert, C. Thomsen, R.D. Jensen and M. Arentoft, *Journal of Materials Processing Technology*, 2009, vol. 209, pp. 1570-1579.
- [26] J.A. Bardt, G.R. Bourne, T.L. Schmitz, J.C. Ziegert and W.G. Sawyer, *J. Mater. Res.*, 2007, vol. 22, pp. 339-343.
- [27] J.J. He, N. Li, N. Tang, X.Y. Wang, C. Zhang and L. Liu, *Intermetallics*, 2012, vol. 21, pp. 50-55.
- [28] J. Schroers, Q. Pham and A. Desai , *Journal of Microelectromechanical Systems*, 2007, vol. 16, pp. 240-247.
- [29] N. Chen, H. A. Yang, A. Caron, P. C. Chen, Y. C. Lin, D. V. Louzguine-Luzgin, K. F. Yao, M. Esashi and A. Inoue, *J Mater Sci*, 2011, vol. 46, pp. 2091–2096.

- [30] G. Kumar, A. Desai and J. Schroers, *Adv. Mater.*, 2011, vol. 23, pp. 461–476.
- [31] N.H. Pryds, *Mat. Sci. Eng. A*, 2004, vol. 186, pp. 375-377.
- [32] M. Carmo, R.C. Sekol, S. Ding, G. Kumar, J. Schroers and A.D. Taylor, *ACS Nano*, 2011, vol. 5, pp. 2979-2983.
- [33] B. Sarac, G. Kumar, T. Hodges, S. Ding, A. Desai and J. Schroers, *Journal of Microelectromechanical Systems*, 2011, vol. 20, pp. 28-36.
- [34] A. Wiest, J. S. Harmon, M. D. Demetriou, R. D. Conner and W. L. Johnson, *Scripta Mater.*, 2009, vol. 60, pp. 160-163.
- [35] M. D. Demetriou, M.E. Launey, G. Garrett, J.P. Schramm, D.C. Hofmann, W. L. Johnson and R.O. Ritchie, *Nature Materials*, 2011, vol. 10, pp. 123-128.
- [36] A.L. Greer, *Nature Materials*, 2011, vol.10, pp. 88-89.
- [37] K. Fujita, Y. Morishita, N. Nishiyama, H. Kimura and A. Inoue, *Materials Transactions*, 2005 vol. 46, pp. 2856-2863.
- [38] M. Bakkal and V. Naksiler, *Materials and Manufacturing Processes*, 2009, vol. 24, pp. 1249–1255.
- [39] S. H. Yeo, P.C. Tan, E. Aligiri, S.B. Tor and N.H. Loh, *Materials and Manufacturing Processes*, 2009, vol. 24, pp. 1242–1248.
- [40] J.A. Koza, R. Sueptitz, M. Uhlemann, L. Schultz and A. Gebert, *Intermetallics*, 2011, vol. 19, pp. 437-444.
- [41] S.N. Aqida, D Brabazon, S. Naher, Z. Kovacs and D.J. Browne, *Applied Physics A: Materials Science & Processing*, 2010, vol. 101, pp. 357-360.
- [42] Y. Yang, J.C. Ye, J. Lua, F.X. Liu and P.K. Liaw, *Acta Materialia*, 2009, vol. 57, pp. 1613–1623.
- [43] B. W. Zhou, X. G. Zhang, W. Zhang, H. Kimura, T. Zhang, A. Makino and A. Inoue, *Materials Transactions*, 2010, Vol. 51, pp. 826 to 829.
- [44] W. Kai, I.F. Ren, P.C. Kao, R.F. Wang, C.-P. Chuang, M.W. Freels and P.K. Liaw, *Advanced Engineering Materials*, 2009, vol. 11, pp. 380-386.
- [45] W. Kai, T.H. Ho, H.H. Hsieh, Y.R. Chen, D.C. Qiao, F. Jiang, G. Fan and P.K. Liaw, *Metall. Mater. Trans. A*, 2009, vol. 39A, pp. 1838-1846.
- [46] J.L. Zhang, W.H. Cao and C. H. Shek, *J. Alloys Comps.*, 2011, vol. 509S, S219-S222.

Figure Captions

Fig.1 (a) Photoresist laid down on silicon wafer, (b) Deep reaction ion etch and remove photoresist, (c) emboss silicon into BMG above glass transition temperature of BMG, (d) remove silicon by dissolution, (e) use BMG as tool to emboss a polymer at temperature below glass transition temperature of BMG, (f) withdraw BMG tool from polymer. Using this route allows a single silicon master to produce one BMG tool which can then produce Y number of plastic components.

Fig.2 (a) Photoresist laid down on silicon wafer, (b) Deep reaction ion etch and remove photoresist, (c) emboss silicon into BMG #1 above glass transition temperature of BMG #1, (d) remove silicon by dissolution, (e) use BMG #1 as tool to emboss multiple tools from BMG#2 with a glass transition temperature below BMG#1, (f) BMG#2 removed and ready to be stand-alone polymer embossing tool, (g) emboss multiple plastic parts with BMG#2 tool at temperature below glass transition temperature of BMG#2, (h) final polymeric parts with small scale features. Using this route allows a single silicon master to produce X BMG tools, which each in turn can produce Y polymeric components (single silicon master produces X x Y polymeric components).

Fig.3 SEM images of a mould patterned with a trough by wire electrical discharge machining (EDM). Note the relatively rough surface finish in the trough.

Fig. 4 (a) SEM images of laser machined holes in $Zr_{47}Cu_{45}Al_8$ BMG. Holes in the image on the left are filled partially with carbon adhesive for imaging. (b) Trench produced in $Zr_{44}Cu_{40}Al_8 Ag_8$ using Trumpf Trumicro Pico second laser is approximately 21 μm wide and 1.5 μm deep in single pass, 30%power (Left image) 40%power (middle) and 50% on the right image.

Fig. 5 (a) SEM images of a logo FIB milled onto $ZrCuAl$ BMG and an OFHC copper plate where the same FIB machining was attempted. (b) SEM images of a gear wheel FIB milled onto $ZrCuAl$ BMG and a piece of microcrystalline tool steel where the same FIB machining was attempted.

Fig. 6: (a) Array of pillars FIB milled into BMG tooling insert, (b) resultant impression on surface of micro injection molded HDPE component [5].

Fig. 7: Ridge replication quality dependence on polymer flow direction (FD): molded height versus feature width [10].

Fig. 8: replication via embossing of sub-microfluidic patterns and micro-UCD crest in PMMA [6].

Fig. 9 Use of silicon master mould to emboss a BMG sub-master and then use of the BMG to emboss PMMA. Images are taken on a Zygo white light interferometer. a) mold with hexagonal structures on a single plane b) mold with hexagonal structures on two different planes.

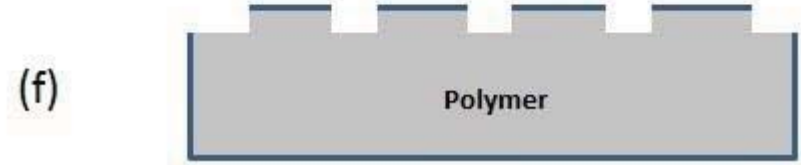
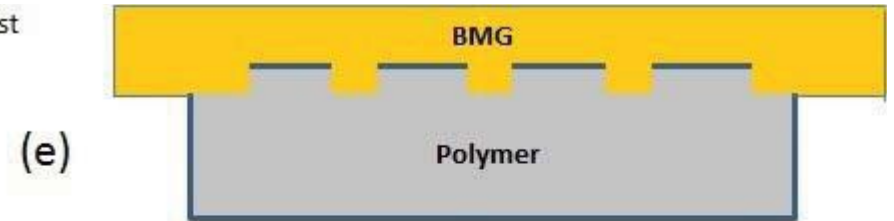


Fig.1 (a) Photoresist laid down on silicon wafer, (b) Deep reaction ion etch and remove photoresist, (c) emboss silicon into BMG above glass transition temperature of BMG, (d) remove silicon by dissolution, (e) use BMG as tool to emboss a polymer at temperature below glass transition temperature of BMG, (f) withdraw BMG tool from polymer. Using this route allows a single silicon master to produce one BMG tool which can then produce Y number of plastic components.

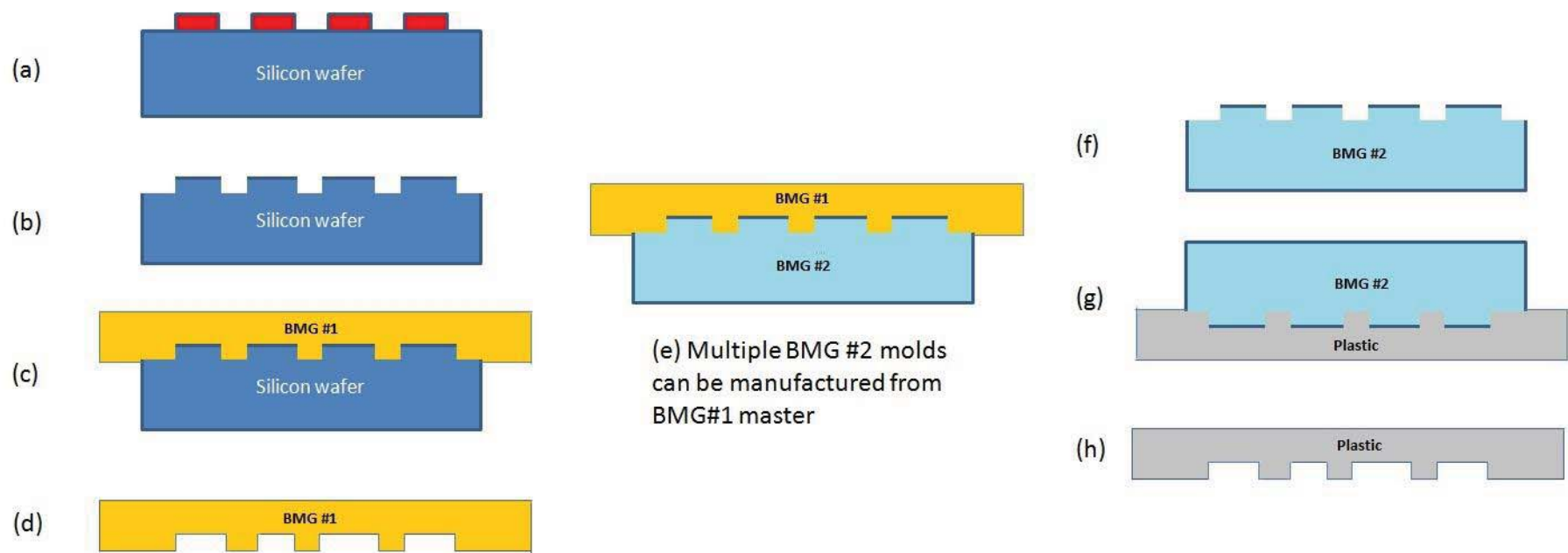


Fig.2 (a) Photoresist laid down on silicon wafer, (b) Deep reaction ion etch and remove photoresist, (c) emboss silicon into BMG #1 above glass transition temperature of BMG #1, (d) remove silicon by dissolution, (e) use BMG #1 as tool to emboss multiple tools from BMG#2 with a glass transition temperature below BMG#1, (f) BMG#2 removed and ready to be stand-alone polymer embossing tool, (g) emboss multiple plastic parts with BMG#2 tool at temperature below glass transition temperature of BMG#2, (h) final polymeric parts with small scale features. Using this route allows a single silicon master to produce X BMG tools, which each in turn can produce Y polymeric components (single silicon master produces X x Y polymeric components).

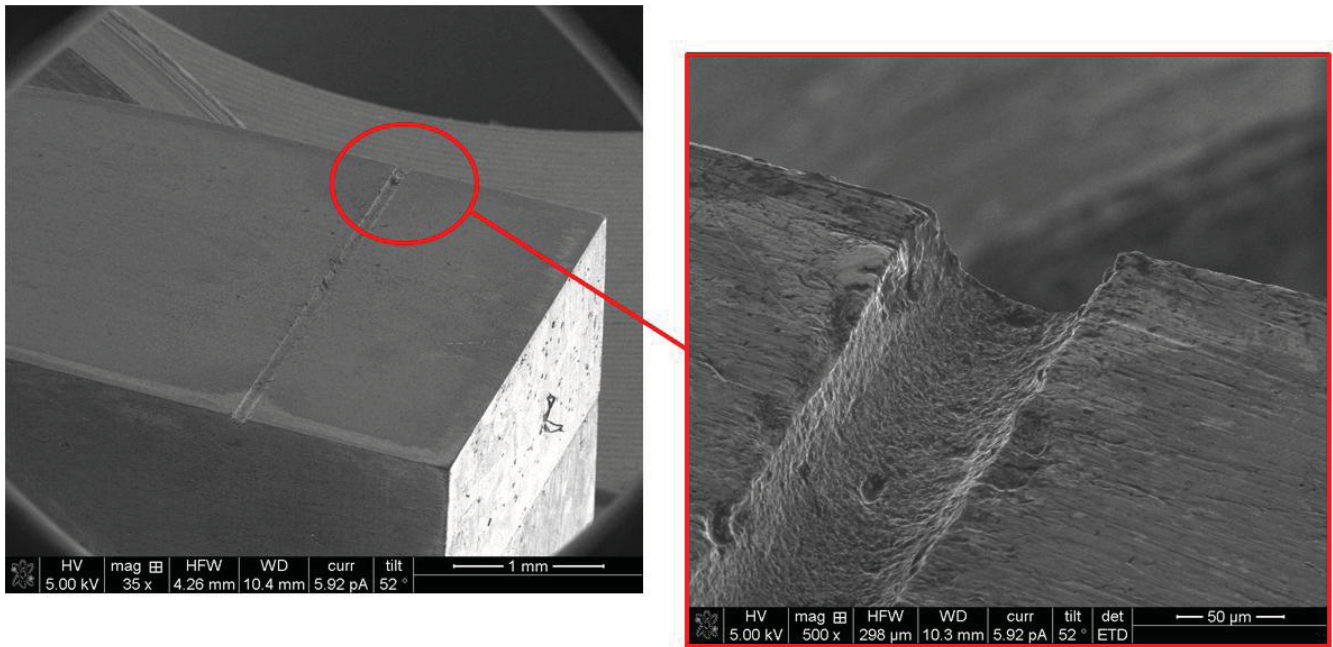


Fig.3 SEM images of a mould patterned with a trough by wire electrical discharge machining (EDM). Note the relatively rough surface finish in the trough.

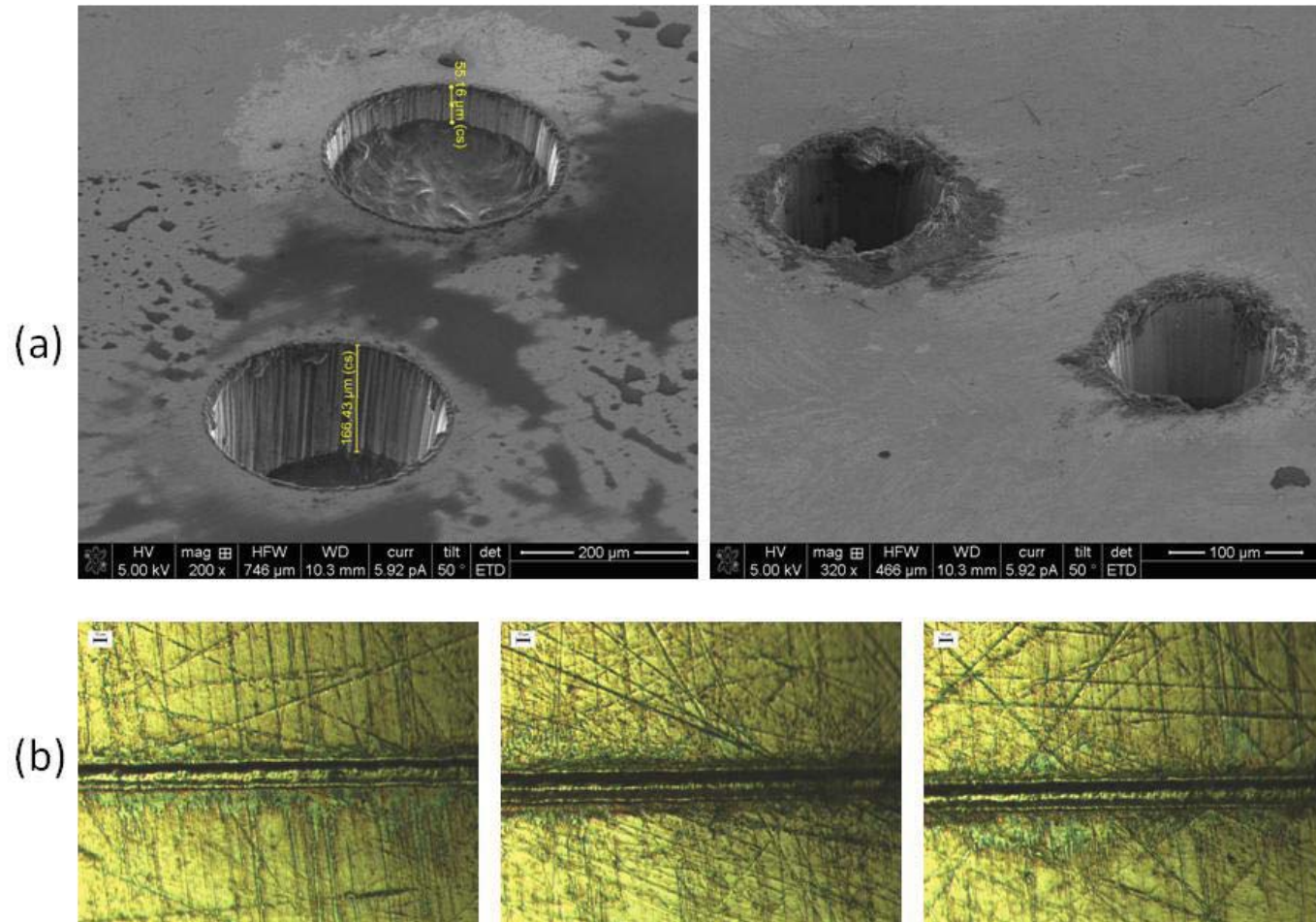


Fig. 4 (a) SEM images of laser machined holes in $Zr_{47}Cu_{45}Al_8$ BMG. Holes in the image on the left are filled partially with carbon adhesive for imaging. (b) Trench produced in $Zr_{44}Cu_{40}Al_8Ag_8$ using Trumpf Trumicro Pico second laser is approximately 21 μm wide and 1.5 μm deep in single pass, 30%power (Left image) 40%power (middle) and 50% on the right image.

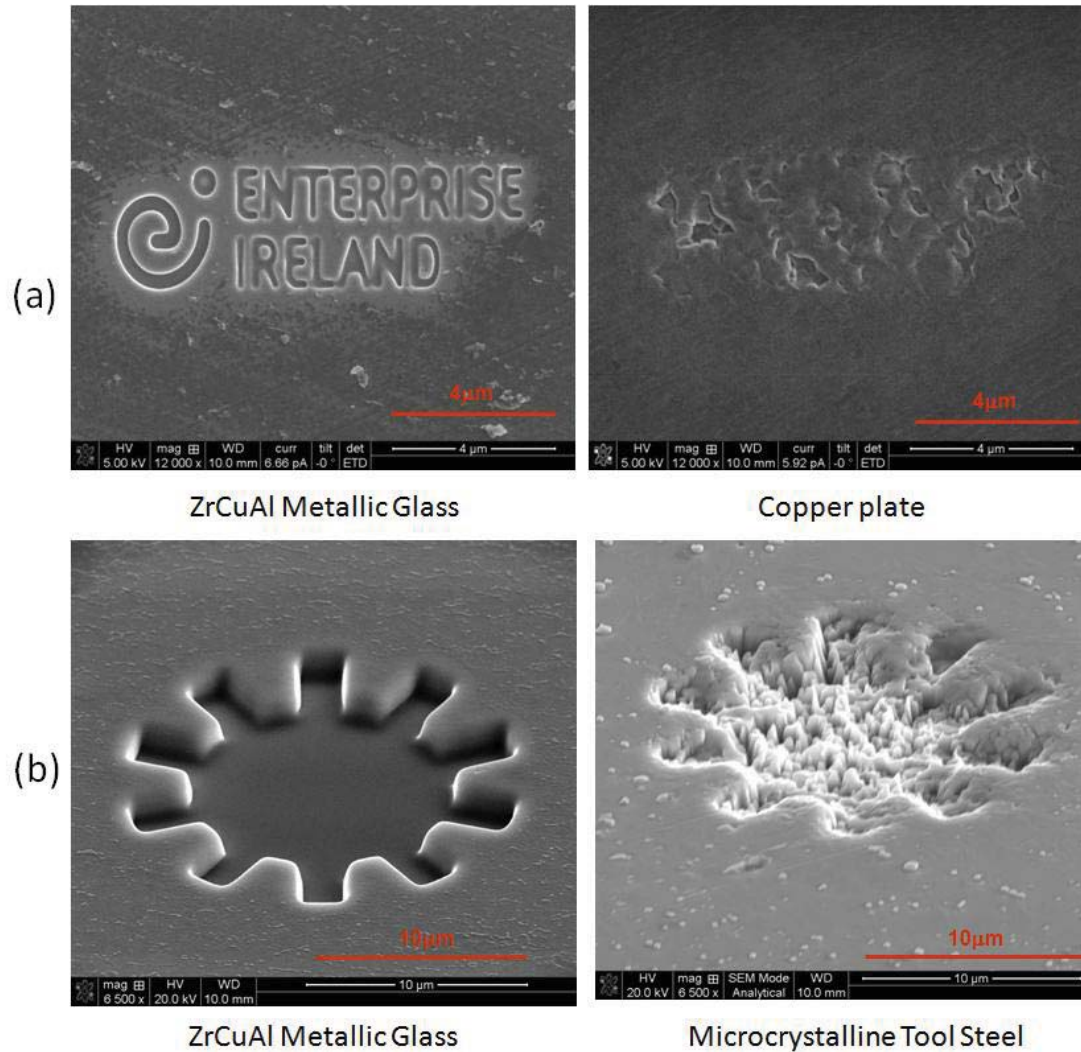
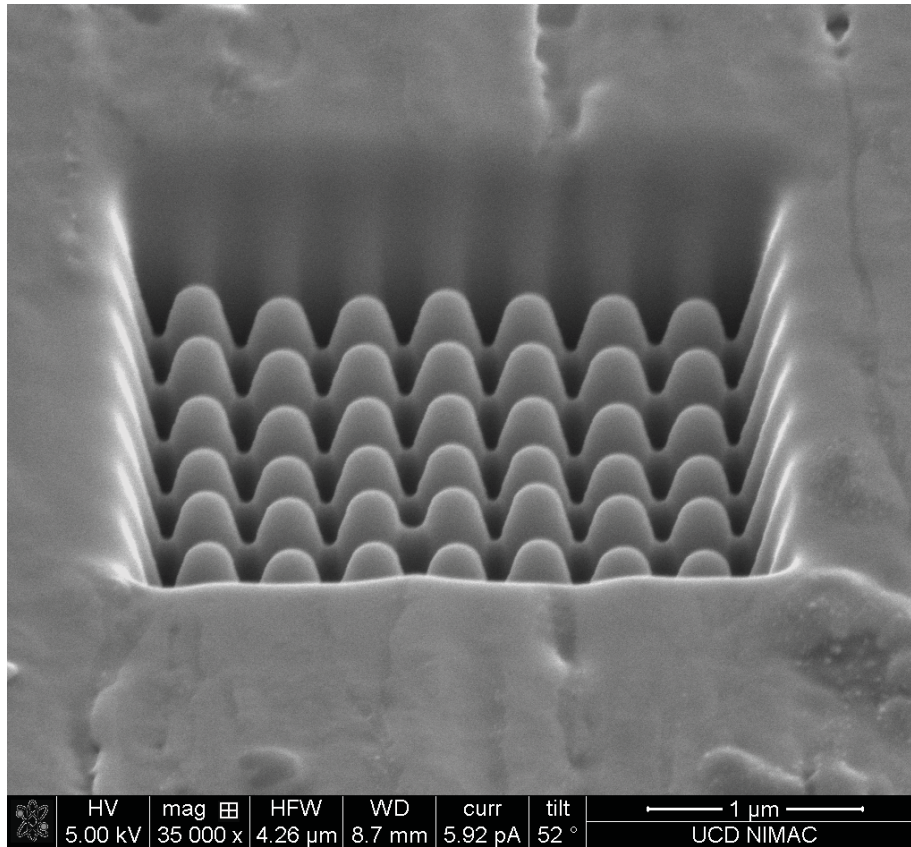


Fig. 5 (a) SEM images of a logo FIB milled onto ZrCuAl BMG and an OFHC copper plate where the same FIB machining was attempted. (b) SEM images of a gear wheel FIB milled onto ZrCuAl BMG and a piece of microcrystalline tool steel where the same FIB machining was attempted.

(a)



(b)

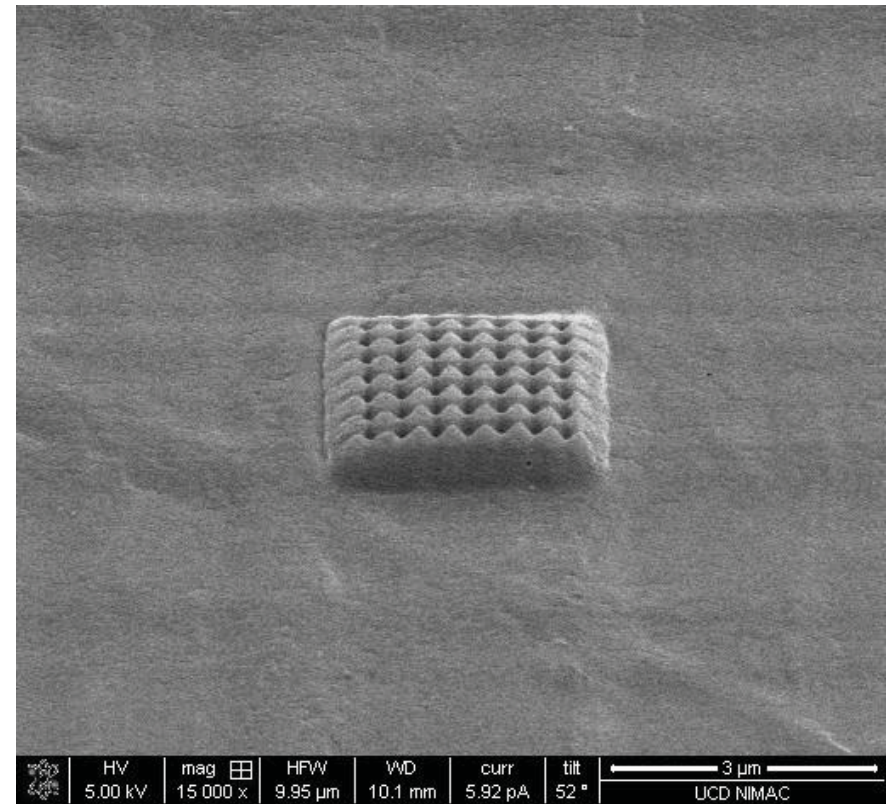


Fig. 6: (a) Array of pillars FIB milled into BMG tooling insert, (b) resultant impression on surface of micro injection molded HDPE component [5].

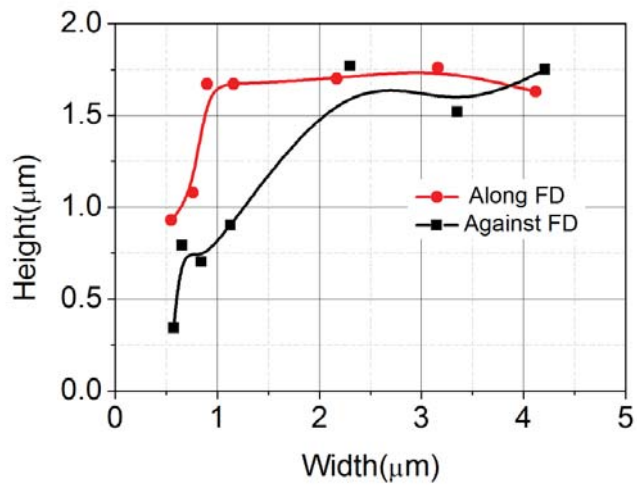
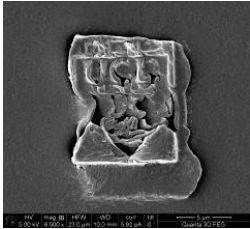
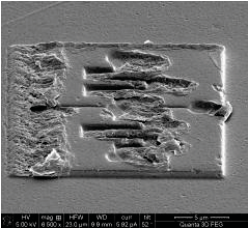
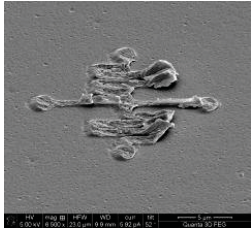
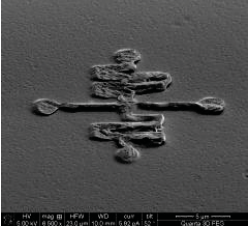
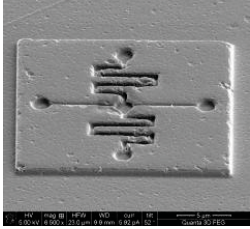
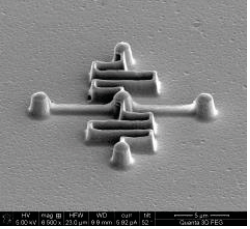
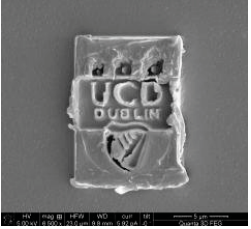
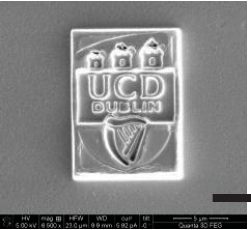
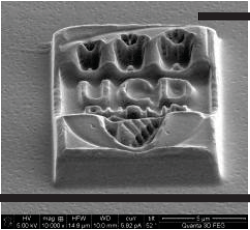
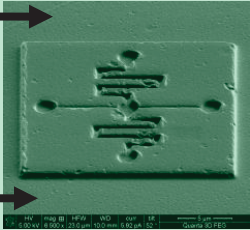
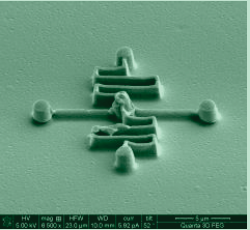
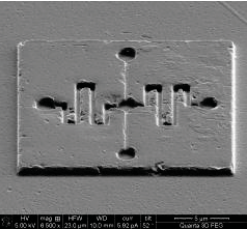
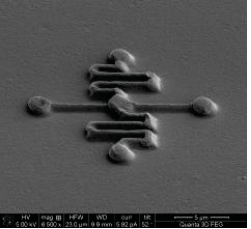
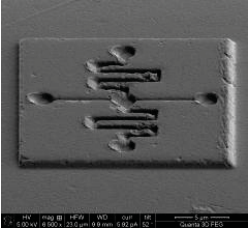
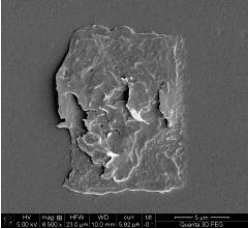


Fig. 7: Ridge replication quality dependence on polymer flow direction (FD): molded height versus feature width [10].

Fig. 8: replication via embossing of sub-microfluidic patterns and micro-UCD crest in PMMA [6].

	110°C	120°C	130°C
1.5 MPa			 
2.0 MPa		 	
2.5 MPa	 	 	
3.0 MPa	 		

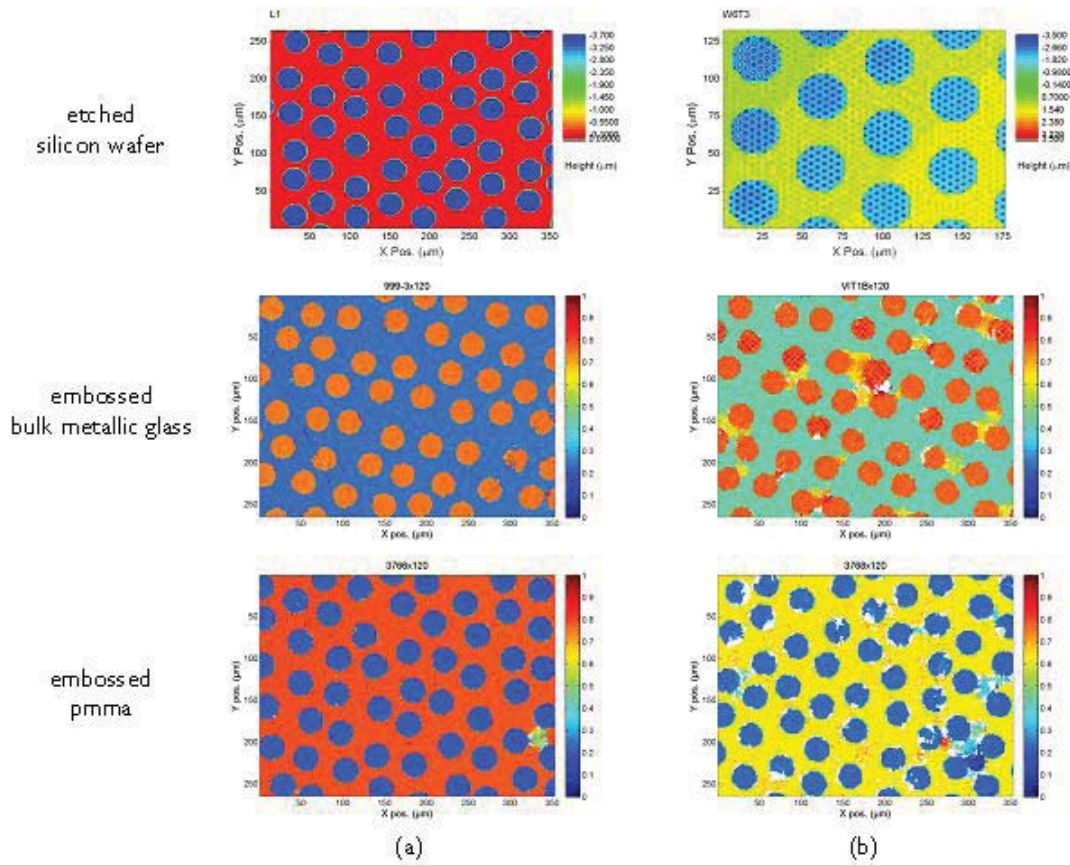


Fig. 9 Use of silicon master mould to emboss a BMG sub-master and then use of the BMG to emboss PMMA. Images are taken on a Zygo white light interferometer. a) mold with hexagonal structures on a single plane b) mold with hexagonal structures on two different planes.